minerals

MDPI

Article

Natural Magnetite Minerals Enhance 1,2-Dichloroethane Reductive Dechlorination

Patrícia Leitão [1,2,3], Matteo Tucci [1], Carolina Cruz Viggi [1], Henri Nouws [3], Anthony S. Danko [2] and Federico Aulenta [1,*]

[1] Water Research Institute (IRSA), National Research Council (CNR), Via Salaria km. 29.300, 00015 Monterotondo (RM), Italy; tichaleitao@hotmail.com (P.L.); matteo.tucci@irsa.cnr.it (M.T.); carolina.cruzviggi@irsa.cnr.it (C.C.V.)
[2] Department of Mining Engineering, University of Porto, Rua Dr. Roberto Frias, 4200-465 Porto, Portugal; asdanko1@gmail.com
[3] REQUIMTE, Institute of Engineering of Porto, Polytechnic Institute of Porto, Rua Dr. António Bernardino de Almeida, 431, 4200-072 Porto, Portugal; han@isep.ipp.pt
* Correspondence: federico.aulenta@irsa.cnr.it

Abstract: Contamination of soil and groundwater by chlorinated solvents is an environmental issue of primary concern. Recently, electrically conductive iron particles have been proposed as a novel approach to accelerate anaerobic bioremediation processes. In fact, it was demonstrated that conductive particles facilitate the exchange of electrons between microorganisms via Direct Interspecies Electron Transfer (DIET) processes, thus enhancing the pollutant-degrading potential of the microbial community. However, the use of natural minerals in this context has not been reported so far. In this study, we applied, for the first time, natural magnetite and hematite to accelerate the reductive dechlorination of 1,2-dichloroethane by an enrichment culture in lab-scale anaerobic microcosms. After four feeding cycles, low magnetite-amended microcosms (13 mg/L) yielded the highest rate of 1,2-DCA reductive dechlorination and reduced methanogenic activity. By contrast, hematite did not display any apparent stimulatory effect. Surprisingly, in the presence of higher amounts of iron oxides, a weaker effect was obtained, probably because iron(III) present in the minerals competed for the electrons necessary for reductive dechlorination. For all microcosms, the concentration of the toxic byproduct vinyl chloride was negligible throughout the whole study. The SEM/EDS analysis confirmed the close interaction between the conductive iron oxide particles and the dechlorinating bacteria. This work opens the possibility of using natural conductive minerals for bioremediation applications as well as shedding light on the previously unrecognized role of such minerals in contaminated ecosystems.

Keywords: magnetite; hematite; conductive particles; reductive dechlorination; groundwater remediation; direct interspecies electron transfer (DIET); 1,2-dichloroethane

Citation: Leitão, P.; Tucci, M.; Cruz Viggi, C.; Nouws, H.; Danko, A.S.; Aulenta, F. Natural Magnetite Minerals Enhance 1,2-Dichloroethane Reductive Dechlorination. *Minerals* **2022**, *12*, 816. https://doi.org/10.3390/min12070816

Academic Editor: Naoko Okibe

Received: 9 May 2022
Accepted: 24 June 2022
Published: 26 June 2022

1. Introduction

1,2-Dichloroethane (1,2-DCA) is a widespread chlorinated aliphatic hydrocarbon (CAH) mostly used as a degreasing agent and a precursor to produce polyvinylchloride (PVC) plastics. Due to incorrect handling, storage and disposal practices, it is often found in soil and groundwater [1]. In subsurface environments, especially after contamination events, molecular oxygen is usually scarce or completely unavailable [2]. In this context, 1,2-DCA needs to be removed either via chemical or biological reductive dechlorination under anaerobic conditions.

Reductive dechlorination of 1,2-DCA may follow alternative pathways (Figure 1): (i) direct dichloroelimination to harmless ethene, a reaction that involves the simultaneous removal of the two chlorine substituents from the contaminant and the formation of a double bond between the two carbon atoms; (ii) dehydrochlorination to vinyl chloride (VC),

a non-redox reaction occurring spontaneously in aqueous systems. This latter reaction can be followed by a reductive hydrogenolysis step (i.e., involving the replacement of the chlorine substituent with hydrogen), resulting in the transformation of VC into ethene [3]. While dehydrochlorination is typically an abiotic reaction, the dichloroelimination and the hydrogenolysis pathways can be catalyzed by so-called organohalide respiring bacteria (OHRB), which thrive using CAHs as respiratory electron acceptors and hydrogen or acetate as electron donors. The most well-studied OHRB belongs to the genus *Dehalococcoides* [4,5], *Dehalobacter* [6] and *Desulfitobacterium* [7,8].

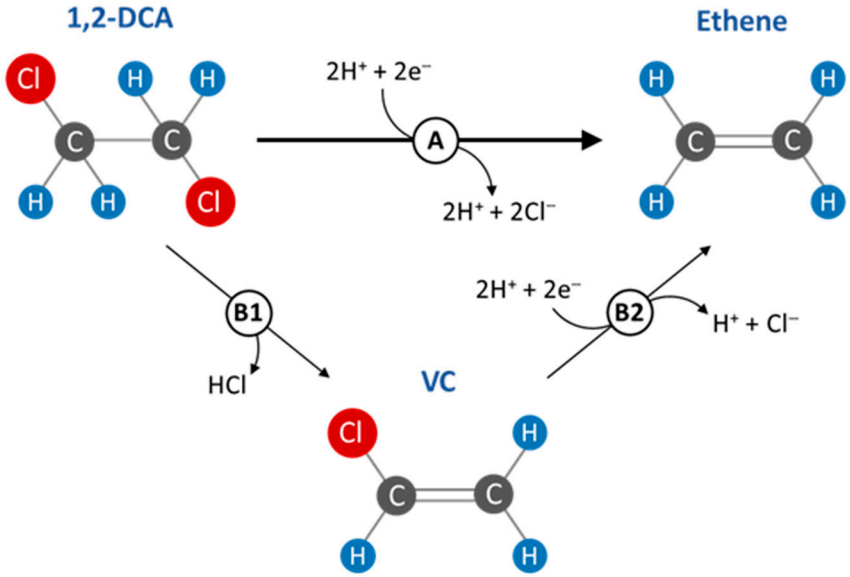

Figure 1. Different degradation pathways of 1,2-DCA: (**A**) dichloroelimination; (**B1**) Dehydrochlorination; (**B2**) Reductive hydrogenolysis. Steps (**A**) and (**B2**) are driven by microorganisms, while (**B1**) is an abiotic reaction.

A typical strategy for 1,2-DCA remediation relies on in situ biostimulations of such dechlorinating microorganisms. As compared to other technologies, this approach benefits from generally lower costs and higher environmental sustainability [9]. It usually involves the injection of fermentable electron donors, such as acetate, lactate, citrate, glycerol, etc., directly into the subsurface of the contaminated site [10]. In this context, several recent studies reported that the addition of electrically conductive minerals such as magnetite or hematite could improve the degradation process by facilitating the electron transfer between microorganisms [11,12] in the so-called direct interspecies electron transfer (DIET) [13]. Indeed, several microorganisms can use conductive or redox active minerals as electron acceptors or donors for extracellular respiration [14], natural batteries for electron storage [15], or electrical conduits for intercellular electron transfer [16].

It was proven that magnetite stimulated the reductive dechlorination of CAHs (e.g., trichloroethene) using acetate as an electron donor [17,18]. In a recent study, we demonstrated that magnetite nanoparticles enhanced the syntrophic reductive dechlorination of 1,2-DCA to ethene up to 3.3-times compared to unamended controls, while decreasing the lag time by 0.8 times (i.e., 23 days) [19]. This is because magnetite facilitated the syntrophic interaction between acetate oxidizing bacteria and halorespiring microorganisms by shuttling electrons from the first to the second. Whilst much work can be found in the literature on the use of "synthetic" iron oxides, very few focused on natural samples [20], which, however, may possess distinctly different surface properties with respect to their lab-synthesized counterpart [21]. To the best of the authors' knowledge, the application of natural electrically conductive minerals to the bioremediation of chlorinated compounds has not been explored so far.

Along this line, it is worth mentioning that the chemical synthesis of magnetite or hematite nanoparticles is a complex and expensive procedure that requires several steps and produces a fair amount of waste, thus making the use of synthetic iron (nano)particles for "real world" applications unsustainable from an environmental and economic standpoint. Herein, natural magnetite and hematite minerals sampled in the north of Portugal were evaluated for their capability of enhancing 1,2-DCA reductive dechlorination in bench-scale microcosms.

2. Materials and Methods

2.1. Magnetite and Hematite Minerals

Natural magnetite (Fe_3O_4) and hematite (α-Fe_2O_3) minerals were sampled in the Northeast region of Portugal, the first one in Marão and the second in Moncorvo (Figure 2). The minerals were kindly offered from the collection of the Mining Engineering Department of the Faculty of Engineering from the University of Porto (Portugal).

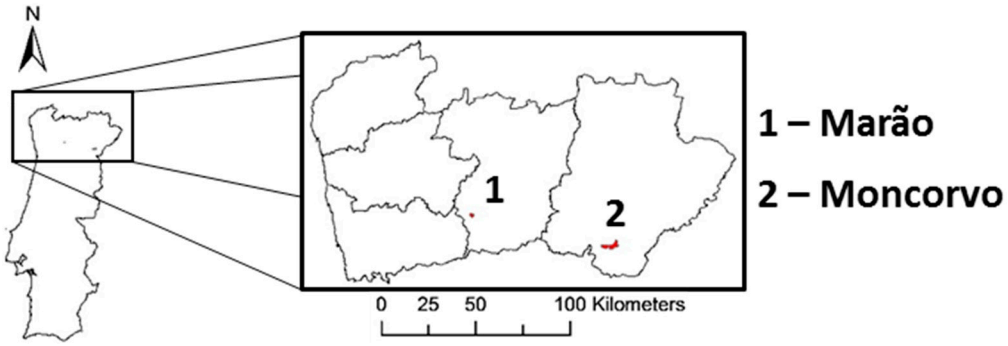

Figure 2. Identification of the origin in Portugal from magnetite and hematite minerals used for this experiment.

The minerals were pretreated by grinding for 15 min in a Siebtechnik laboratory disc mill (SIEBTECHNIK TEMA, Mülheim an der Ruhr, Germany). Particle size analysis was performed by the laser diffraction particle size analyzer Malvern Mastersizer 2000 (Malvern Panalytical Ltd., Marvern, UK) coupled with the dispersion unit Hydro2000G (Malvern Panalytical Ltd., Marvern, UK). Samples were dispersed in water, combined with agitation and ultrasound when needed to separate aggregates. Elemental composition was determined by the X-ray fluorescence X-MET7500 (Oxford Instruments, Abingdon, UK).

2.2. 1,2-DCA-Dechlorinating Mixed Microbial Culture

The inoculum used for the experiments was an anaerobic electroactive culture previously enriched in an H-type bioelectrochemical cell with 1,2-DCA as electron acceptor and a polarized (−900 mV vs. the standard hydrogen electrode) graphite rod serving as the sole electron donor [22]. Prior to being used, the culture was transferred into an anaerobic serum bottle (120 mL of total volume and 95 mL of liquid volume), sealed with Teflon-faced butyl rubber stoppers. This bottle was operated in a semi-batch mode through sequential feedings with 1,2-DCA (0.05 mmol) and H_2 (0.8 mmol) on a weekly basis. Prior to each new feeding, the headspace of the bottle was flushed with N_2 to remove volatile compounds (i.e., the remaining 1,2-DCA, its dechlorination products and methane), and a fixed volume of liquid phase was replaced with a fresh medium to maintain the average hydraulic retention time at approximately 30 days. Before usage in this experiment, 4.5 hydraulic retention times passed.

2.3. Microcosm Setup

The experiments were conducted in 120 mL serum bottles sealed with Teflon-faced butyl rubber stoppers that were flushed with N_2 to establish anaerobic conditions. Table 1 shows the experimental conditions in each microcosm setup. All microcosms were incu-

bated upside down, in the dark, at 25 °C under mild agitation, with acetate (10 mM) and 1,2-DCA (approximately 0.45 mM).

Table 1. Experimental setup of the microcosms.

	Magnetite Control	Hematite Control	Unamended	Magnetite Low	Magnetite	Hematite
Inoculum (mL)	/	/	4	4	4	4
Magnetite (mg)	5.3 ± 0.3	/	/	1.2 ± 0.3	5.3 ± 0.3	/
Hematite (mg)	/	5.3 ± 0.3	/	/	/	5.3 ± 0.3

The total liquid volume in the microcosms was 90 mL, and each treatment was performed in duplicate. The medium contained the following components: NH_4Cl (0.5 g/L), $MgCl_2 \cdot 6H_2O$ (0.1 g/L), K_2HPO_4 (0.4 g/L), $CaCl_2 \cdot 2H_2O$ (0.05 g/L), trace metal solution (10 mL/L) [23], vitamin solution (10 mL/L) [24] and $NaHCO_3$ (15 mL/L, 10% *w*/*v*). The pH value of the medium was around 7.5. All microcosms were operated in a semi-batch regime, consisting of repeated feeding cycles, each with an average duration of approximately 20 days. At the beginning of each feeding cycle, the microcosms were purged with N_2 for 10 min to remove volatile compounds and maintain anaerobic conditions. Then, a fixed volume of liquid phase was replaced with a fresh anaerobic medium containing acetate (10 mM), with a resulting average hydraulic retention time of approximately 120 days. The concentration of acetate, which served both as an oxidizable substrate and carbon source for biomass growth, was maintained in excess during the whole experiment. Then, 10 mL of CO_2 was added to the headspace of each bottle, along with a given amount of 1,2-DCA. Throughout the study, all microcosms were analyzed daily to quantify the residual 1,2-DCA, the reductive dechlorination products, methane and acetate, as described in the following paragraph.

2.4. Analytical Methods

Volatile components, namely 1,2-DCA, vinyl chlorine (VC), ethene (ETH) and methane (CH_4), were quantified by injecting 50 µL of headspace (taken with a gas-tight locked syringe) into a Shimadzu GC-2014 gas chromatograph (2.4 m × 2.1 mm packed column 60/80 Carbopack B/1% SP-1000; N_2 carrier gas 40 mL/min; oven temperature 60 °C with an increment of 40 °C per min until 180 °C; flame ionization detector temperature 200 °C).

To determine the total amount of each volatile compound present in the bottles, headspace and liquid phase concentrations were calculated using tabulated Henry's law constants [25]. At the end of the experiments, samples were analyzed by SEM/EDS to study the spatial distribution and the morphology of microorganisms and the iron oxide particles. Sample pre-treatment and analysis were carried out as detailed previously [19]. All samples were viewed with FEI Quanta 400FEG ESEM/EDAX Genesis X4M (FEI Company, Hillsboro, OR, USA) in high-vacuum mode at 10 or 15 kV. X-ray microanalysis was performed in specific fields of the samples for elemental analysis.

For each feeding cycle, the RD rate and CH_4 production rate (both expressed as meq/L d) were calculated from the measured amounts of ETH and CH_4, respectively, and considering that 2 mol of electrons (meq) are needed for the formation of 1 mol of ETH from 1,2-DCA and 8 meq are needed for the formation of 1 mol CH_4 from CO_2.

An unpaired *t*-test (Graphpad software, San Diego, CA, USA) was used to compare values and assess the statistical significance of observed differences.

3. Results and Discussion

3.1. Natural Magnetite and Hematite Characterization

Particle size and elemental composition of the natural magnetite and hematite used as amendments in the microcosms were analyzed by means of laser diffraction and X-ray fluorescence, respectively. From the granulometric curves presented in Figure 3A, it can be

observed that magnetite minerals have a larger grain size compared to hematite, where 80% of hematite particles are ≤9.5 µm, while for magnetite, 80% of particles are ≤26 µm.

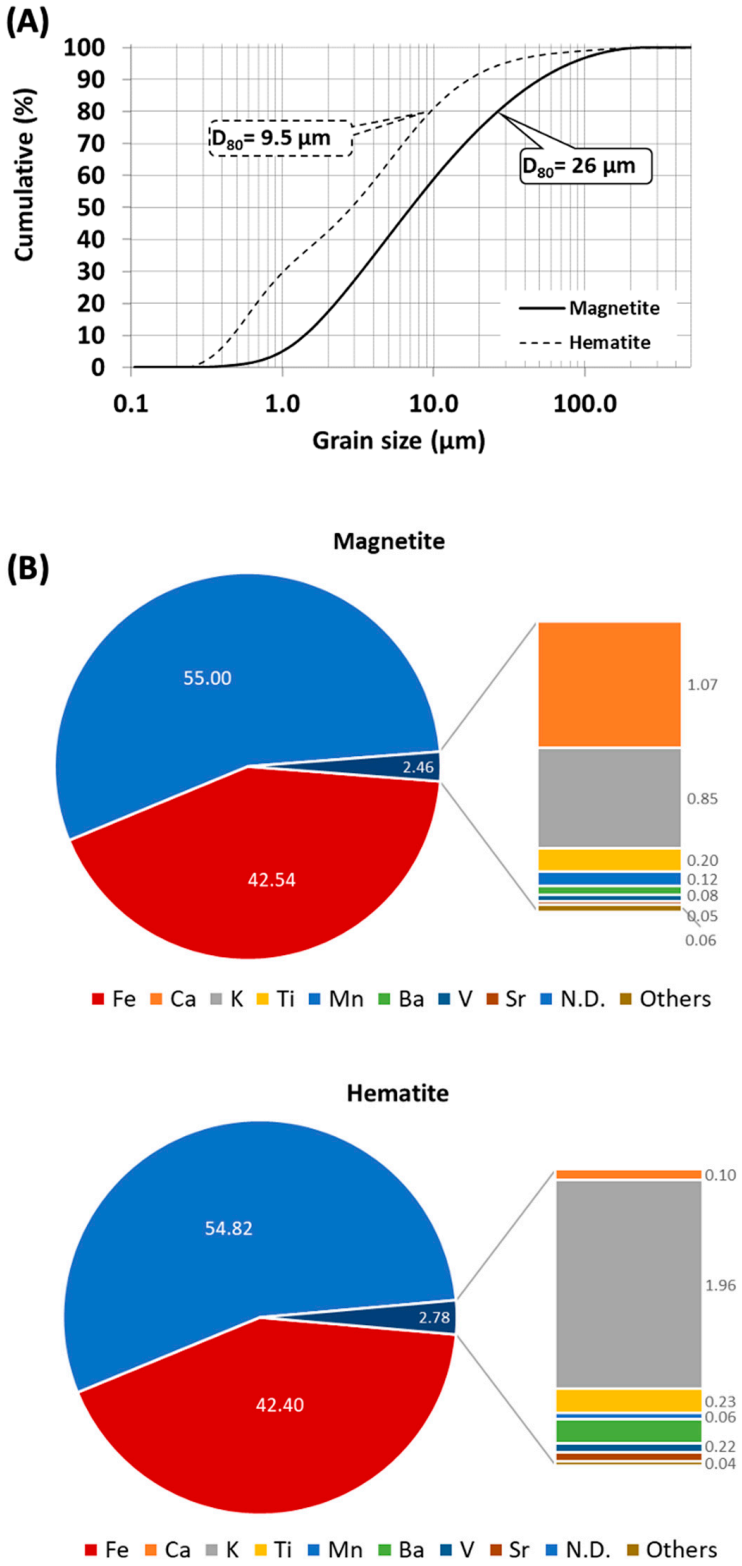

Figure 3. Characterization of the natural magnetite and hematite in terms of (**A**) particle size and (**B**) elemental composition of used minerals.

Regarding the elemental composition, as expected, both minerals present a similar percentage of iron, which is about 42% on a mass basis. The percentage of unidentified elements (N.D.) is about 55% for both samples. In all likelihood, this number mostly accounts for oxygen, which is a constituent part of both minerals. Among the other elements, calcium, potassium, titanium, manganese and barium were the most abundant in the analyzed samples.

3.2. Influence of Magnetite and Hematite on Anaerobic Dechlorination

The effect of iron mineral supplementation on dechlorination of 1,2-DCA and competitive methane production was evaluated (Figure 4). During the 80 days of experimentation, four feeding cycles were performed, each lasting about 20 days.

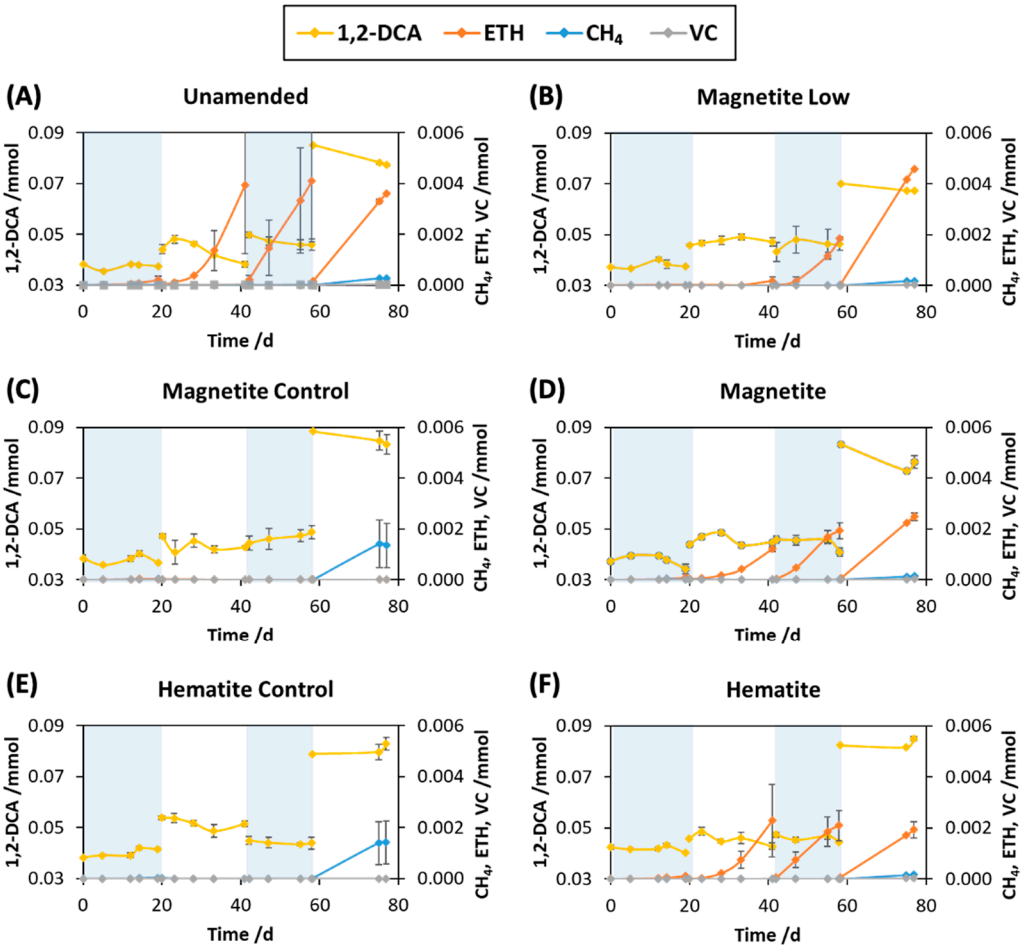

Figure 4. Trends of 1,2-DCA, ETH, VC and CH_4 for all treatments, namely: (**A**) Unamended control; (**B**) Magnetite low; (**C**) Non-inoculated Magnetite control; (**D**) Magnetite; (**E**) Non-inoculated Hematite control; (**F**) Hematite. The values are obtained as average of two replicates.

It can be noticed how the dechlorination process during the first cycle is almost negligible in all treatments. This finding is likely due to the fact that the inoculated culture used hydrogen as a direct electron donor for 1,2-DCA dechlorination, whereas acetate was herein supplied. Starting from the second cycle, the decrease in the total amount of 1,2-DCA in the bottles and the production of ethene can clearly be observed in all inoculated microcosms (Figure 4A,B,D,F), while no indication of dechlorinating activity was found in the non-inoculated controls (Figure 4C,E).

The reductive dechlorination (RD) products measured in the microcosms consist primarily of ethene, and the presence of VC remains negligible throughout the whole study. Accordingly, the direct dichloroelimination pathway (Figure 1A) seems to be prevalent

relative to the dehydrochlorination route (leading to the formation of VC), with this latter being eventually followed by the reductive hydrogenolysis of VC to ethene (Figure 1B). The one-step conversion of toxic 1,2-DCA into ethene without the intermediate formation and/or accumulation of VC is a positive outcome for the remediation process since this latter compound is far more toxic and dangerous than its parent compound [26].

The RD products formation rate increased as the experiment progressed for all inoculated microcosms (Figure 5A). In the first three feeding cycles, the unamended microcosms had the highest RD rates; however, in the last feeding cycle, the best performance was clearly observed for the microcosms amended with 1.2 mg of magnetite (Magnetite Low), which displayed a substantially ($p < 0.05$) higher RD rate. For the experiments amended with natural iron oxides, the lag time preceding the onset of dechlorination was substantially longer with respect to the unamended control.

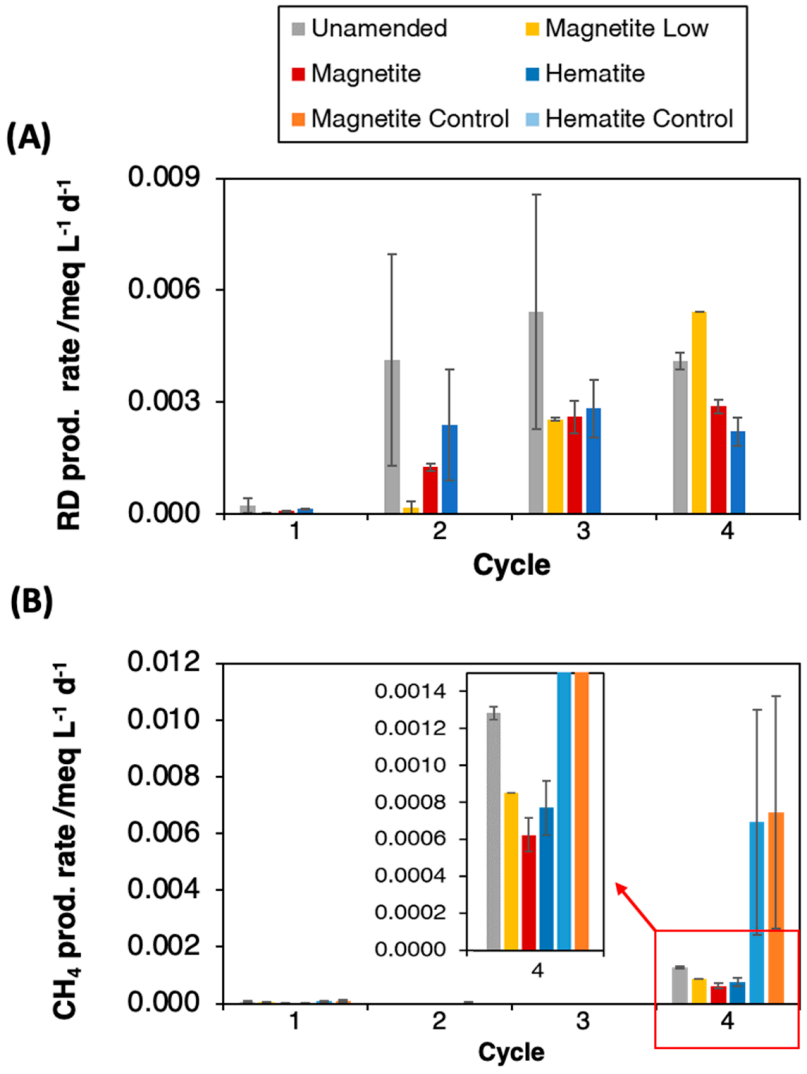

Figure 5. For each treatment during the different feeding cycles: (**A**) average RD production rate; (**B**) CH_4 generation.

This result is in contrast with previous findings related to the use of synthetic magnetite nanoparticles, with these latter reducing the lag time for dechlorination by about 20% [19]. It is possible that impurities present on the natural magnetite and hematite and the larger particle size reduce the affinity between the minerals and bacterial cells. Moreover, other mineral characteristics, such as crystallinity, stoichiometry, surface properties, etc., may also have influenced the DIET-based stimulatory effect [20]. Among the different treatments, it

can be noticed that the microcosm amended with a lower amount of magnetite (Magnetite Low) outperformed both the microcosms amended with a higher amount of magnetite (Magnetite) and with hematite during the last cycle. This phenomenon can be explained by the fact that Fe(III) present in magnetite and hematite can be biologically reduced to Fe(II) [20]. Thus, when the concentration of these minerals becomes too high, they may start to compete for the electrons resulting from acetate degradation, which are then diverted away from the dechlorinating metabolism. Since the iron in hematite is solely Fe(III), its negative impact on the RD production rate is likely more pronounced than the one of magnetite, which instead contains both Fe(II) and Fe(III). Along this line, some studies pointed out that Fe and Mn minerals may cause inhibition of CAH dechlorination as they can represent energetically more favorable terminal electron acceptors [27].

In all microcosms, methanogenesis starts during the last feeding cycle. The methanogenic activity competes with the RD since it also exploits the reducing power deriving from acetate degradation. Indeed, methane generation was about one order of magnitude higher in the controls, where no dechlorination was taking place (Figure 5B). Moreover, all amended microcosms showed a significantly lower methane production as compared to the Unamended ones. This fact could be a reason why the Magnetite Low microcosms outperformed the Unamended ones during the last cycle: the instauration of the competing methanogenic pathway negatively affected the RD production rate more strongly in the Unamended microcosms with respect to the Magnetite Low ones.

Notably, the observed methane production in non-inoculated "abiotic" treatments was most probably triggered by "biological" reactions that were established, after a long period of operation, in the bottles since they were neither autoclaved at the start of the study nor operated under strictly sterile conditions.

3.3. Scanning Electron Microscopy and Energy-Dispersive X-ray Spectroscopy Analysis

At the end of the experiments, samples from the treatments amended with magnetite and hematite were analyzed by SEM/EDS to study the spatial distribution and the morphology of microorganisms and the iron oxide particles (Figure 6).

In the SEM images, it is possible to observe the presence of some conductive iron oxide particles associated with the cell membrane of microorganisms for both the magnetite and the hematite samples. The disc-shaped bacterial cells shown in Figure 6A resemble the morphology of the OHRB *Dehalococcoides mccartyi*, although the apparent length of cells (>1.8 μm) is substantially larger than that reported in the literature for this microorganism [28]. Indeed, these bacteria are probably the ones responsible for the observed RD process in the microcosms.

From the EDS spectrum Z1 depicted in Figure 6A, it is possible to see that the main elements present are carbon, nitrogen, oxygen, and sodium, confirming that analysis was performed on a microorganism. Iron and iron precipitates are not present; thus, the microorganisms did not incorporate magnetite into the cell wall.

The spectra Z2 in Figure 6A and Z1 and Z2 in Figure 6B all present an iron oxide peak, which confirms the presence of magnetite and hematite particles. Overall, these findings suggest that bacterial cells were likely utilizing iron oxide particles as a conductive network to exchange electrons. The Si peak present in all spectra is most likely due to the contamination of the samples, which may have occurred during the preparation procedure.

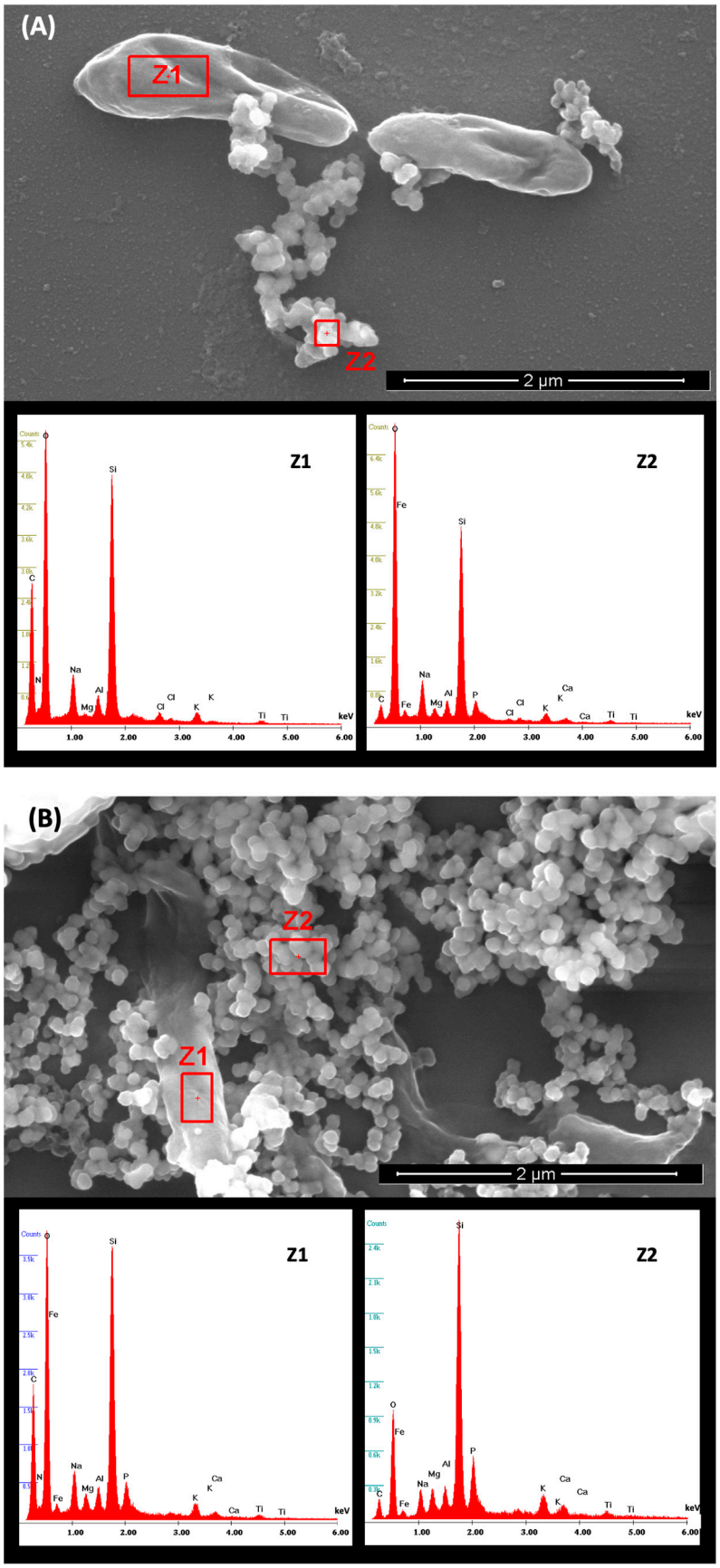

Figure 6. SEM image from microcosms: (**A**) magnetite, (**B**) hematite and EDS analysis corresponding to the areas Z1 and Z2 outlined in red.

4. Conclusions

This study investigated the application of natural, electrically conductive iron oxide minerals to accelerate the anaerobic bioremediation of 1,2-DCA in lab-scale microcosms. Low amounts of magnetite yielded the best performance in terms of dechlorination rate, particularly upon long-term operation. Indeed, in such microcosms, the RD rate significantly increased over the whole experimental period, whereas in other treatments, the RD rate either peaked in correspondence of the third cycle (in unamended controls and magnetite supplemented microcosms) or increased far more slowly (in hematite supplemented microcosms). In accordance with previous studies carried out using synthetic magnetite particles, the stimulatory effect is possibly derived from the capacity of such minerals to promote a DIET-based process between acetate-degrading microorganisms and dechlorinating bacteria. Additionally, in microcosms supplemented with low amounts of magnetite, the establishment of a competitive methanogenic route was less pronounced with respect to the other treatments. Interestingly, higher amounts of magnetite and hematite were not beneficial to the reductive dechlorination of 1,2-DCA, probably because the reduction in Fe(III) present in the minerals competed for the electrons necessary for the pollutant removal.

Finally, SEM imaging coupled with EDS analysis confirmed the close interplay between dechlorinating bacteria and conductive iron oxide minerals. This work paves the way for the implementation of natural conductive minerals for the bioremediation of chlorinated compounds. Further studies should investigate the longer-term effect of iron oxide minerals on the microbial communities present in the contaminated soil, as well as the optimization of the conductive mineral dosage.

Author Contributions: Conceptualization, P.L., A.S.D. and F.A.; validation, M.T.; formal analysis, P.L.; investigation, P.L.; resources, A.S.D. and F.A.; data curation, P.L. and M.T.; writing—original draft preparation, review and editing M.T. and F.A.; visualization, C.C.V.; supervision, H.N., A.S.D. and F.A.; funding acquisition, A.S.D. and F.A. All authors have read and agreed to the published version of the manuscript.

Funding: The authors would like to thank FCT (Portuguese Foundation for Science and Technology) for the financial support of Patrícia Leitão through the Ph.D. grant SFRH/BD/87312/2012.

Acknowledgments: The authors would like to thank CEMUP-Centro de Materiais da Universidade do Porto for expert assistance and helpful discussions about SEM measurements.

Conflicts of Interest: The authors declare no conflict of interest. The funders had no role in the design of the study; in the collection, analyses, or interpretation of data; in the writing of the manuscript, or in the decision to publish the results.

References

1. Dinglasan-Panlilio, M.J.; Dworatzek, S.; Mabury, S.; Edwards, E. Microbial Oxidation of 1,2-Dichloroethane under Anoxic Conditions with Nitrate as Electron Acceptor in Mixed and Pure Cultures. *FEMS Microbiol. Ecol.* **2006**, *56*, 355–364. [CrossRef] [PubMed]
2. Lovley, D.R. Bioremediation: Anaerobes to the Rescue. *Science* **2001**, *293*, 1444–1446. [CrossRef] [PubMed]
3. Schmidt, M.; Lege, S.; Nijenhuis, I. Comparison of 1,2-Dichloroethane, Dichloroethene and Vinyl Chloride Carbon Stable Isotope Fractionation during Dechlorination by Two Dehalococcoides Strains. *Water Res.* **2014**, *52*, 146–154. [CrossRef]
4. Duhamel, M.; Edwards, E.A. Growth and Yields of Dechlorinators, Acetogens, and Methanogens during Reductive Dechlorination of Chlorinated Ethenes and Dihaloelimination of 1,2-Dichloroethane. *Environ. Sci. Technol.* **2007**, *41*, 2303–2310. [CrossRef]
5. He, J.; Ritalahti, K.M.; Yang, K.-L.; Koenigsberg, S.S.; Löffler, F.E. Detoxification of Vinyl Chloride to Ethene Coupled to Growth of an Anaerobic Bacterium. *Nature* **2003**, *424*, 62–65. [CrossRef]
6. Grostern, A.; Edwards, E.A. Characterization of a Dehalobacter Coculture That Dechlorinates 1,2-Dichloroethane to Ethene and Identification of the Putative Reductive Dehalogenase Gene. *Appl. Environ. Microbiol.* **2009**, *75*, 2684–2693. [CrossRef] [PubMed]
7. Maes, A.; Van Raemdonck, H.; Smith, K.; Ossieur, W.; Lebbe, L.; Verstraete, W. Transport and Activity of Desulfitobacterium Dichloroeliminans Strain DCA1 during Bioaugmentation of 1,2-DCA-Contaminated Groundwater. *Environ. Sci. Technol.* **2006**, *40*, 5544–5552. [CrossRef]

8. Marzorati, M.; De Ferra, F.; Van Raemdonck, H.; Borin, S.; Allifranchini, E.; Carpani, G.; Serbolisca, L.; Verstraete, W.; Boon, N.; Daffonchio, D. A Novel Reductive Dehalogenase, Identified in a Contaminated Groundwater Enrichment Culture and in Desulfitobacterium Dichloroeliminans Strain DCA1, Is Linked to Dehalogenation of 1,2-Dichloroethane. *Appl. Environ. Microbiol.* **2007**, *73*, 2990–2999. [CrossRef]
9. Zhang, S.; Hou, Z.; Du, X.M.; Li, D.M.; Lu, X.X. Assessment of Biostimulation and Bioaugmentation for Removing Chlorinated Volatile Organic Compounds from Groundwater at a Former Manufacture Plant. *Biodegradation* **2016**, *27*, 223–236. [CrossRef]
10. Chen, M.; Tong, H.; Li, F.; Liu, C.; Lan, Q.; Liu, C. The Effect of Electron Donors on the Dechlorination of Pentachlorophenol (PCP) and Prokaryotic Diversity in Paddy Soil. *Eur. J. Soil Biol.* **2018**, *86*, 8–15. [CrossRef]
11. Lovley, D.R. Syntrophy Goes Electric: Direct Interspecies Electron Transfer. *Annu. Rev. Microbiol.* **2017**, *71*, 643–664. [CrossRef] [PubMed]
12. Zhuang, L.; Tang, Z.; Ma, J.; Yu, Z.; Wang, Y.; Tang, J. Enhanced Anaerobic Biodegradation of Benzoate under Sulfate-Reducing Conditions with Conductive Iron-Oxides in Sediment of Pearl River Estuary. *Front. Microbiol.* **2019**, *10*, 374. [CrossRef] [PubMed]
13. Aulenta, F.; Tucci, M.; Cruz Viggi, C.; Dolfing, J.; Head, I.M.; Rotaru, A.E. An Underappreciated DIET for Anaerobic Petroleum Hydrocarbon-Degrading Microbial Communities. *Microb. Biotechnol.* **2020**, *14*, 2–7. [CrossRef] [PubMed]
14. Melton, E.D.; Swanner, E.D.; Behrens, S.; Schmidt, C.; Kappler, A. The Interplay of Microbially Mediated and Abiotic Reactions in the Biogeochemical Fe Cycle. *Nat. Rev. Microbiol.* **2014**, *12*, 797–808. [CrossRef]
15. Byrne, J.M.; Klueglein, N.; Pearce, C.; Rosso, K.M.; Appel, E.; Kappler, A. Redox Cycling of Fe(II) and Fe(III) in Magnetite by Fe-Metabolizing Bacteria. *Science* **2015**, *347*, 1473–1476. [CrossRef]
16. Shi, L.; Dong, H.; Reguera, G.; Beyenal, H.; Lu, A.; Liu, J.; Yu, H.Q.; Fredrickson, J.K. Extracellular Electron Transfer Mechanisms between Microorganisms and Minerals. *Nat. Rev. Microbiol.* **2016**, *14*, 651–662. [CrossRef]
17. Aulenta, F.; Fazi, S.; Majone, M.; Rossetti, S. Electrically Conductive Magnetite Particles Enhance the Kinetics and Steer the Composition of Anaerobic TCE-Dechlorinating Cultures. *Process Biochem.* **2014**, *49*, 2235–2240. [CrossRef]
18. Aulenta, F.; Rossetti, S.; Amalfitano, S.; Majone, M.; Tandoi, V. Conductive Magnetite Nanoparticles Accelerate the Microbial Reductive Dechlorination of Trichloroethene by Promoting Interspecies Electron Transfer Processes. *ChemSusChem* **2013**, *6*, 433–436. [CrossRef]
19. Leitão, P.; Aulenta, F.; Rossetti, S.; Nouws, H.P.A.; Danko, A.S. Impact of Magnetite Nanoparticles on the Syntrophic Dechlorination of 1,2-Dichloroethane. *Sci. Total Environ.* **2018**, *624*, 17–23. [CrossRef]
20. You, Y.; Zheng, S.; Zang, H.; Liu, F.; Liu, F.; Liu, J. Stimulatory Effect of Magnetite on the Syntrophic Metabolism of Geobacter Co-Cultures: Influences of Surface Coating. *Geochim. Cosmochim. Acta* **2019**, *256*, 82–96. [CrossRef]
21. Salazar-Camacho, C.; Villalobos, M.; de la Luz Rivas-Sánchez, M.; Arenas-Alatorre, J.; Alcaraz-Cienfuegos, J.; Gutiérrez-Ruiz, M.E. Characterization and Surface Reactivity of Natural and Synthetic Magnetites. *Chem. Geol.* **2013**, *347*, 233–245. [CrossRef]
22. Leitão, P.; Rossetti, S.; Danko, A.S.; Nouws, H.; Aulenta, F. Enrichment of *Dehalococcoides mccartyi* Spp. from a Municipal Activated Sludge during AQDS-Mediated Bioelectrochemical Dechlorination of 1,2-Dichloroethane to Ethene. *Bioresour. Technol.* **2016**, *214*, 426–431. [CrossRef] [PubMed]
23. Zeikus, J.G. The Biology of Methanogenic Bacteria. *Bacteriol. Rev.* **1977**, *41*, 514–541. [CrossRef]
24. Balch, W.E.; Fox, G.E.; Magrum, L.J.; Woese, C.R.; Wolfe, R.S. Methanogens: Reevaluation of a Unique Biological Group. *Microbiol. Rev.* **1979**, *43*, 260–296. [CrossRef]
25. Gossett, J.M. Measurement of Henry's Law Constants for Hydrocarbons. *Environ. Sci. Technol.* **1987**, *21*, 202–208. [CrossRef]
26. Kielhorn, J.; Melber, C.; Wahnschaffe, U.; Aitio, A.; Mangelsdorf, I. Vinyl Chloride: Still a Cause for Concern. *Environ. Health Perspect.* **2000**, *108*, 579–588. [CrossRef]
27. Zaa, C.L.Y.; McLean, J.E.; Dupont, R.R.; Norton, J.M.; Sorensen, D.L. Dechlorinating and Iron Reducing Bacteria Distribution in a TCE-Contaminated Aquifer. *Groundw. Monit. Remediat.* **2010**, *30*, 46–57. [CrossRef]
28. Löffler, F.E.; Yan, J.; Ritalahti, K.M.; Adrian, L.; Edwards, E.A.; Konstantinidis, K.T.; Müller, J.A.; Fullerton, H.; Zinder, S.H.; Spormann, A.M. *Dehalococcoides mccartyi* Gen. Nov., Sp. Nov., Obligately Organohalide-Respiring Anaerobic Bacteria Relevant to Halogen Cycling and Bioremediation, Belong to a Novel Bacterial Class, *Dehalococcoidia* Classis Nov., Order Dehalococcoidales Ord. Nov. and family Dehalococcoidaceae fam. nov., within the phylum *Chloroflexi*. *Int. J. Syst. Evol. Microbiol.* **2013**, *63*, 625–635. [CrossRef]